Materials Characterization 120 (2016) 337–344

Contents lists available at ScienceDirect

Materials Characterization

journal homepage: www.elsevier.com/locate/matchar

A study of the deformation and failure mechanisms of protective intermetallic coatings on AZ91 Mg alloys using microcantilever bending

Mingyuan Lu, James Mead, Yueqin Wu, Hugh Russell, Han Huang *

School of Mechanical and Mining Engineering, The University of Queensland, QLD 4072, Australia

ARTICLE INFO

Article history:
Received 22 June 2016
Received in revised form 1 September 2016
Accepted 13 September 2016
Available online 14 September 2016

Keywords:
Mg alloy
Interface
Microcantilever
Nanoindentation
FIB milling

ABSTRACT

In this study, a nanoindentation-based microcantilever bending technique was utilized to investigate the interfacial properties of a β-$Mg_{17}Al_{12}$/AZ91 Mg alloy film/substrate system under tensile loading conditions. Finite element analysis (FEA) was first undertaken to optimise the design of cantilever structures for inducing high tensile stresses at the interface. Cantilevers consisting of a necked region or notch at the interface were determined to be the most successful designs. Microcantilevers containing the β-$Mg_{17}Al_{12}$/AZ91 interface were then made using focused ion beam (FIB) milling technique. Necks were made in the cantilevers to intensify the tension at the interface and notches were used to introduce a stress concentration to the interface. During bending, the cantilevers were deflected to failure. Subsequent analysis of the deformed cantilevers using electron microscopies revealed that plastic deformation, and subsequent ductile rupture, of the AZ91 phase was the dominant failure mechanism. When the β-$Mg_{17}Al_{12}$/AZ91 film/substrate system was subjected to tension, the softer AZ91 phase failed prior to interfacial delamination, demonstrating that the strength of the interface exceeded the stresses that caused ductile failure in the substrate material.

1. Introduction

The widespread application of Mg alloys is hindered by their susceptibility to wear and corrosion, which could deleteriously influence the reliability of Mg-based structural components used under abrasive and corrosive service conditions [1,2]. Surface modification is an effective way to enhance surface durability of the alloys without influencing their bulk mechanical properties, and hence is widely applied to various Mg alloys [3,4]. Among the existing surface modification techniques, Al diffusion coating (aluminising) has been recognised as a promising approach to enhance wear and corrosion resistance of Mg alloys [5–9]. Through aluminising treatment, hard and inert intermetallic compounds were formed on the surface of the alloys, providing protection from wear and corrosion [9–12]. A packed powder diffusion coating (PPDC) technique using Al and Zn mixed powders as the diffusion source was successfully applied to obtain thick polycrystalline β-$Mg_{17}Al_{12}$ and τ-$Mg_{32}(Al, Zn)_{49}$ intermetallic layers on Mg alloys. This process has proven to be effective at providing protection from both wear and corrosion for Mg alloys [6,13]. The intermetallic layers exhibited high hardness (approximately a fourfold increase over bulk Mg [14]) and the corrosion resistance of both β-$Mg_{17}Al_{12}$ and τ-$Mg_{32}(Al, Zn)_{49}$ phases in NaCl solution was found to be one to two orders of magnitude higher than that of AZ91 Mg alloys [6,9,15]. The β-$Mg_{17}Al_{12}$ and τ-$Mg_{32}(Al, Zn)_{49}$ protective layers were also found to exhibit impressively high fracture strengths of 1.76 GPa and 1.05 GPa respectively [16].

To ensure the reliability of Mg alloys, the protective coatings must adhere well to the substrate to prevent it from being exposed to atmosphere [17]. Delamination of the coating from the Mg alloy substrate could lead to localised oxidation corrosion, which would subsequently cause failure of the protective coatings. During processing or service, stress (tension in particular) being generated at the film/substrate interface may cause localised film-substrate separation and then accelerate the detachment of the film from the substrate. Therefore, investigating potential interfacial failure mechanisms of the film/substrate structures is of considerable practical importance.

In our previous study, a methodology for testing the fracture strength of coatings was successfully developed [16]. The technique incorporated a microcantilever bending experimental system with FEA to determine the fracture strength of β-$Mg_{17}Al_{12}$ and τ-$Mg_{32}(Al, Zn)_{49}$ intermetallic coatings. In the present work, FEA was used initially to assist in the design of cantilever geometries containing a β-$Mg_{17}Al_{12}$/AZ91 interface. Using the insights gained from the FEA, focused ion beam (FIB) milling was used to fabricate microcantilevers with different geometries. Nanoindentation was then utilized to bend the cantilevers to failure in order to understand the deformation behaviour of the interface under tension.

* Corresponding author: School of Mechanical and Mining Engineering, The University of Queensland, St Lucia, QLD 4072, Australia.
E-mail address: han.huang@uq.edu.au (H. Huang).

http://dx.doi.org/10.1016/j.matchar.2016.09.020
1044-5803/

2. Experimental and Simulation Details

2.1. Specimens

Cast AZ91 Mg-alloy with chemical composition of 8.31 wt.% Al, 0.52 wt.% Zn, 0.6 wt.% Mn, and 90.57 wt.% Mg was used in this study. Specimens were first cut from the AZ91 ingots, with dimensions of 15 mm × 10 mm × 10 mm and then treated at 413 °C for 18 h using PPDC technique. The details of the PPDC process can be found in [6, 15]. After the treatment, specimens were cross-sectioned, ground and polished. As shown in Fig. 1, the polished specimen has two distinguishable intermetallic layers formed as a result of the PPDC treatment, with τ-$Mg_{32}(Al, Zn)_{49}$ phase being the top layer and β-$Mg_{17}Al_{12}$ phase sandwiched between τ-phase and AZ91 substrate.

2.2. Finite Element Analysis

FEA was used to aid in the design of cantilever geometries that are effective at generating high tensile stresses at the β-$Mg_{17}Al_{12}$/AZ91 interface during bending. 3D linear-elastic symmetric models were developed using ANSYS 16.1. A graduated mesh of 8-node SOLID 185 elements was used. The interface was assumed to be fully coherent with no transition zone. Accordingly, elements on either side of the interface were connected by common nodes, resulting in an abrupt change in properties. The elastic modulus (E) values of β-$Mg_{17}Al_{12}$ and AZ91 phases used in the models were $E_\beta = 73.6$ GPa and $E_{AZ91} = 49.5$ GPa, respectively, which were determined by nanoindentation using a TI900 Hysitron Triboindenter system (Hysitron Inc., Eden Prairie, MN). A Berkovich indenter with an included angle of 142.3° and a tip radius of 100 nm was used in the test. The Poisson's ratios (ν) of β-$Mg_{17}Al_{12}$ and AZ91 used in the model were $\nu_\beta = 0.237$ [18] and $\nu_{AZ91} = 0.29$ [9] respectively.

The simulation results demonstrate that two cantilever designs are most successful at promoting high tensile stresses at the β-$Mg_{17}Al_{12}$/AZ91 interface. For each cantilever design, the orientation of the two phases could be flipped, giving two separate phase configurations. The first design has a neck section at the interface region, as shown in Fig. 2(a). Such a configuration produces elevated tensile stress at the interface through a reduction in cross-section. The bending stress fields at the neck for each phase configuration, designated as cantilevers C1 and C2, are shown in Figs. 3(a) and 3(b), respectively. For C2, a 'compliant' support column was introduced. This modification allowed for the entire cross-section of the neck being placed under tension.

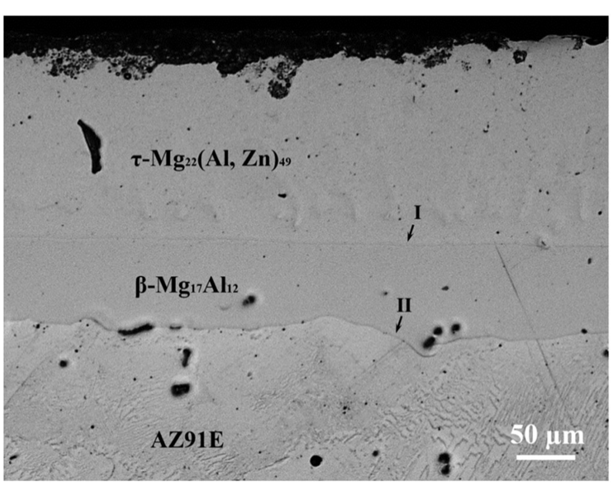

Fig. 1. optical micrograph of the intermetallic layers on a cross-section of a typical PPDC-treated AZ91 Mg alloy sample; arrows I and II indicate the τ-$Mg_{22}(Al, Zn)_{49}$/β-$Mg_{17}Al_{12}$ and β-$Mg_{17}Al_{12}$/AZ91 interfaces respectively.

The second design consists of a sharp notch located precisely at the β-$Mg_{17}Al_{12}$/AZ91 interface, as shown in Fig. 2(b). The stress concentration introduced at the notch provides elevated tensile stresses at the interface. In the models, the widths and root radii of each of the notches were reproduced from the measurements taken from TEM cross-sections of previous FIB-machined notches using the same milling parameters. The bending stress fields at the notch region for each configuration, designated as cantilevers C3 and C4, are shown in Figs. 3(c) and 3(d).

2.3. Focused Ion Beam (FIB) Machining of Cantilevers

Microcantilevers were machined using FIB (FEI Scios DualBeam, Oregon, USA). The detailed cantilever machining process has been reported in our previous study [16]. Fig. 4 shows the cantilevers imaged using a JEOL7100F scanning electron microscope (SEM; JEOL Ltd., Tokyo, Japan). A shallow hole (approximately 50 nm in depth and 600 nm in diameter) locating along the centreline of the cantilever was made to create a well-defined location for placing indentation load and to prevent the spherical tip from sliding during loading. Four cantilevers were machined according to designs identified using FEA. Each cantilever consists of two single-crystalline components of β-$Mg_{17}Al_{12}$ and AZ91, which are separated by an interface. The neck feature at the interfacial region of each of the cantilevers (C1 and C2, Figs. 4(a)–(d)) was milled using 0.1 nA at 30 keV as a final step. The interface notches for cantilevers C3 (Figs. 4(e) and 4(f)) and C4 (Figs. 4(g) and 4(h)) were made using a low milling current (10 pA at 30 keV) to minimize radiation damage to the interface [19–21]. The notches were placed precisely at the β-$Mg_{17}Al_{12}$/AZ91interfaces on the top surface of the cantilevers. After the cantilevers were machined, final polishing using low energy and small current ion beam (2 keV, 0.1 nA) was used to create clean side walls and remove irradiation damaged layers.

2.4. Bending Test

The TI900 Hysitron nanoindentation system was used to apply bending load to the cantilevers. A conical indenter with a spherical apex was used. The tip used has an included angle of 90°; the radius of the spherical apex is 1 μm. During bending, the indenter tip was placed in the shallow hole on the centreline of the beam; the cantilever was then loaded at a rate of 5 nm/s. The deformed cantilevers were subsequently examined using SEM. FIB milling was used to cross-section the deformed cantilevers along the centreline and thin lamella containing the β-$Mg_{17}Al_{12}$/AZ91 interfaces were made for examination using TEM (FEI Tecnai F20, FEI, Oregon, USA).

The FEA models were then updated with the measured geometry of the fabricated cantilevers, and the elastic deflection of the cantilevers was simulated accordingly. The resultant deflection was used to calculate the compliance of the microcantilever C_{FEA}, defined as $C = P/h$. The result was then compared to experimental compliance C_{exp} for validation.

3. Results

3.1. The β-$Mg_{17}Al_{12}$/AZ91interface

TEM examination of the β-$Mg_{17}Al_{12}$/AZ91film/substrate cross-sections identified the interface as the grain and phase boundaries for both phases, as shown in Fig. 5(a). The boundary is often not a straight line, suggesting that the three-dimensional profile of the interface is irregular. Numerous isolated lath-shape precipitates of β-$Mg_{17}Al_{12}$ phase were observed in the AZ91 phase and the continuous precipitations were formed from the presence of supersaturated Mg alloy in the region near to the interface during the PPDC treatment [22,23]. The density of the precipitates declines within 1 μm of the interface, which is likely attributed to the depletion of Al. The Al depletion is the result of Al